

**NOTICE:**

The copyright law of the United States (Title 17, United States Code) governs the making of reproductions of copyrighted material. One specified condition is that the reproduction is not to be "used for any purpose other than private study, scholarship, or research." If a user makes a request for, or later uses a reproduction for purposes in excess of "fair use," that user may be liable for copyright infringement.

**RESTRICTIONS:**

This student work may be read, quoted from, cited, and reproduced for purposes of research. It may not be published in full except by permission of the author.

Matthew F. Georgy

Honors Project Thesis

Feb. 10, 1998

**The Construction of Blue Fluorescent Protein**

Honors Committee Members:

By placing our signatures on this cover page, we hereby deem the Honors Project of Matthew F. Georgy worthy of Biology Departmental Honors.

Dr. Diehl:

Jack D. Diehl

Dr. Newman:

Jeffy Newman

Dr. Mahler:

Oliver H. Mahler

Dr. Fisher:

David G. Fisher

## Abstract

Green Fluorescent Protein (GFP) is a 238-amino acid polypeptide originally isolated from the bioluminescent jellyfish, *Aequoria victoria*. In its wild-type form, the protein exhibits fluorescence excitation and emission maxima of 395 and 508 nm respectively. Fluorescence is mediated by a tripeptide fluorophore which forms via the autocatalytic cyclization and oxidation of three adjacent amino acid residues. The observation that GFP can be expressed in any organism into which it is cloned and without the need for additional enzymes or cofactors has led to its use as a monitor of gene expression and protein localization. Recently, attempts have been made to alter the spectral characteristics of the protein in order to make it useful for a wider variety of applications. The construction of several blue-fluorescing mutants has permitted the simultaneous tracking of different proteins *in vivo*. In my report, I describe the construction of a quadruple mutant blue fluorescent protein which is suitable for cloning into bacteria. Oligonucleotide-mediated site-directed mutagenesis was used to sequentially introduce the necessary codon changes.

## Introduction

Green fluorescent protein (GFP) is a 238-amino acid, 27-kilodalton protein originally isolated from the bioluminescent jellyfish, *Aequoria victoria* (Fig. 1). Its role in nature is as an energy transfer acceptor. When the photoprotein aequorin binds  $\text{Ca}^{2+}$ , it assumes its activated form and catalyzes the oxidation of the molecule coelenterazine to coelenteramide. The latter is in an excited state. Upon returning to its ground state, coelenteramide emits blue light. *In vivo*, however, this chemiluminescent energy is transferred in a radiationless manner to the associated GFP which then emits green fluorescent light (1).

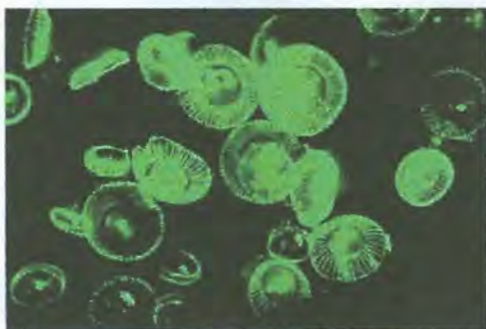


**Fig. 1.** Photograph of *Aequoria victoria*. GFP is responsible for the bioluminescence.

Unlike other fluorescent proteins, which require substrates or cofactors for expression, the fluorescent machinery of GFP is contained entirely within the structure of the apoprotein. Furthermore, the protein attains an actively fluorescent form in an entirely autocatalytic manner. These properties enable GFP to be heterologously expressed in virtually any organism into which it is cloned. It is the first known example of genetically encodable fluorescence (2). The unique properties of GFP have led to its widespread use in the field of cell biology. The fact that 6 N-terminal and 9 C-terminal amino acids can be removed without loss of fluorescence allows

GFP to be expressed as a fusion protein (3). When fused with another protein, it can be used as a monitor of gene expression and as a means of *in vivo* tracking of protein localization. When expressed alone, GFP can be used to follow cell populations or to study infections (4).

Structurally, GFP represents a novel motif which has been named the  $\beta$ -can. The “can” consists of 11  $\beta$ -sheets surrounding a central  $\alpha$ -helix (Fig. 2). This cylindrical structure is 30 Å in width and 40 Å in length, making it much more compact than the common  $\beta$ -barrel motif (5).

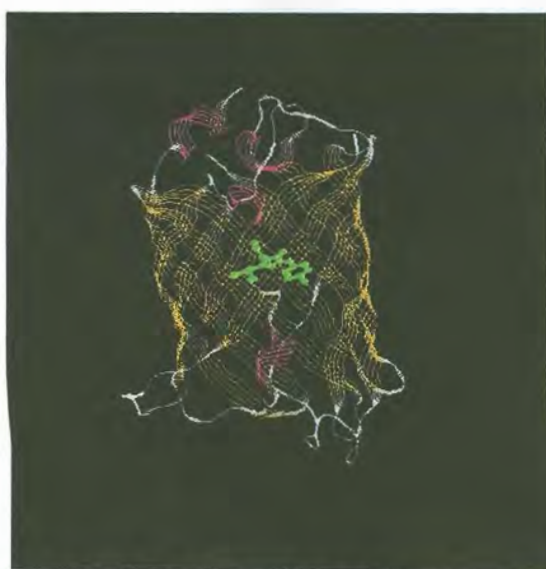


Fig. 2. Diagram of the structure of GFP. The  $\beta$ -strands are indicated in yellow, and the  $\alpha$ -helices in white. The fluorophore is shown as a green ball-and-stick structure

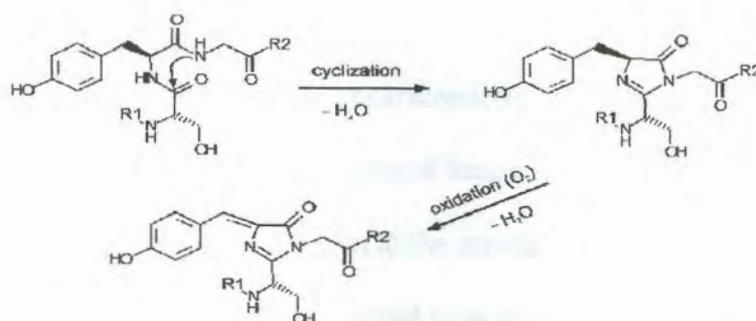


Fig. 3. Proposed mechanism for the formation of the fluorophore.

Lying along the axis of the central  $\alpha$ -helix is a tripeptide fluorophore that forms via the autocatalytic cyclization and oxidation of  $-\text{Ser}^{65}-\text{Tyr}^{66}-\text{Gly}^{67}-$  (Fig. 3). The amino nitrogen of  $\text{Gly}^{67}$  exerts nucleophilic attack on the carbonyl carbon of  $\text{Ser}^{65}$ . Subsequent loss of the carbonyl oxygen as  $\text{H}_2\text{O}$  results in an imidazole ring. The  $\alpha$ -carbon- $\beta$ -carbon bond then undergoes oxidation, completing an extensive  $\pi$ -system (6). This fluorophore is responsible for the fluorescent properties of the protein. Its location within the center of the  $\beta$ -can protects it from small molecules present in the surrounding solvent. In particular, collisional quenching of the excited state due to oxygen is eliminated. In addition to protecting the fluorophore from diffusible ligands, the compact  $\beta$ -can renders GFP highly resistant to denaturation. Fluorescence has been observed to persist in the presence of such chemical denaturants as 6M guanidine HCl, 8M urea, and 1% sodium dodecyl sulfate (SDS). Treatment with 1 mg/mL concentrations of such proteases as trypsin, chymotrypsin, and pancreatin likewise has no effect on fluorescence (5).

The outside of the  $\beta$ -can contains a large number of hydrophilic residues. Such residues are believed to be involved in the formation of a GFP homodimer which has been observed in solutions of low ionic strength. The significance of the dimer is uncertain and it is not known whether it forms *in vivo* (5).

Fluorescence in general is a phenomenon characterized by the absorption of an incident photon followed by subsequent radiation of a photon of longer wavelength. The absorbing molecule passes into the first excited state. Upon return to the ground state, a photon is emitted. In fluorescence terminology, these two events are referred to as excitation and emission respectively.

The wavelength shift is a result of energy lost during the lifetime of excited state, which lasts

from  $10^{-9}$  to  $10^{-4}$  seconds. Molecules containing conjugated  $\pi$ -systems have relatively small gaps between the ground state and the first excited state and are therefore more likely to exhibit fluorescence phenomena (7). The fluorophore of GFP has such a system.

Spectrally, wild-type GFP has an excitation maximum of 395 nm, corresponding to long wavelength UV. A second, smaller excitation peak is present at the blue wavelength of 475 nm. Green fluorescent emission occurs at 508 nm. As GFP is irradiated at its 395 nm maximum, there is a gradual shift in absorption toward the 475 nm peak (8). The presence of two excitation peaks in GFP and the eventual loss of the 395 nm peak can both be explained in terms of alternate ionization states of the phenolic hydroxyl group of Tyr<sup>66</sup>. As the fluorophore absorbs 395 nm light and is promoted to the excited state, the acidity of the phenolic hydrogen increases by several orders of magnitude. Such vast differences in pKa between the ground state and the excited state are a characteristic of many molecules. With the increased acidity, equilibrium shifts toward the deprotonated phenolate conformation. The phenolate form of the fluorophore is responsible for the 475 nm absorption. Additionally, it is the only form that emits light (9).

The rigid encasement and chemical isolation of the fluorophore account for some of the other observed fluorescent properties. The Stokes shift, or difference between the wavelength of emission and excitation, is relatively small for GFP. Because the magnitude of this shift is dependent on the amount of energy which is dissipated during the lifetime of the excited state, such a small shift would be expected for a molecule which undergoes few collisional interactions. For similar reasons, GFP has a high quantum yield, as measured by the ratio of quanta emitted to quanta absorbed (10).

When isolated by proteolytic digestion or *de novo* synthesis, the fluorophore is non-fluoresc-

ent (6). This observation indicates the importance of hydrogen bonding in its spectral properties. When GFP attains its tertiary configuration, numerous hydrophilic amino acid residues are brought into the immediate vicinity of the fluorophore. The presence of these contacts creates an electrostatic environment that permits fluorescent emission (Fig. 4). Such H-bonding-mediated

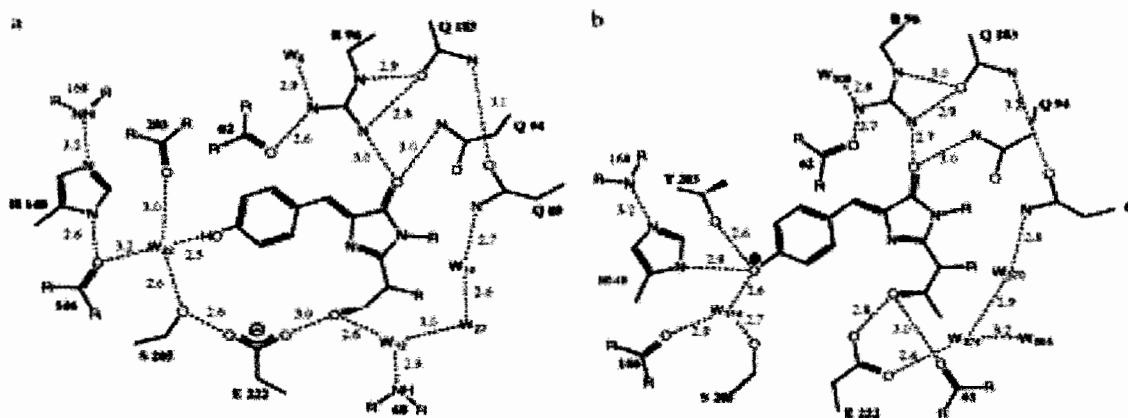


Fig. 4. Diagram showing some of the hydrophilic contacts of the fluorophore. The alternate ionization states of Tyr<sup>66</sup> are indicated as well.

enhancement of fluorescence is observed with many fluorescent molecules as is attributable to a lowering of the relative energy gap between the  $\pi$ -ground and  $\pi$ -excited states (5, 7).

Much research has gone toward the optimization of GFP by making specific amino acid changes. Experimentally, wild-type GFP has some problematic characteristics. Its UV excitation maximum is poorly matched with filter sets and has the potential to be injurious to the organism in which GFP is being expressed. Additionally, its complex photoisomerization results in rapid diminishment of fluorescence (11). In addition to mitigating these factors, mutant forms of GFP with distinct emission and absorption spectra could be used to simultaneously track different proteins, follow differential cell lineages and follow expression of multiple genes. Here, I describe the use of site-directed mutagenesis to construct a blue-emitting GFP variant that is suitable for cloning into bacteria.



## Materials and Methods

**Plasmid isolation.** A strain of *E. coli* containing the gene for the S65T variant of GFP cloned into the *Hind III* site of pTB93F was obtained (12). The cells were inoculated into 5 mL of liquid LB spec. The culture was grown overnight in a 37° C shaking incubator. A 1-mL aliquot of this culture was added to a flask containing 125 mL of LB spec. and the flask incubated overnight at 30° C. Plasmid isolation was done according to the Qiagen® Midiprep protocol. The culture was added to two 50-mL tubes and centrifuged to produce a cell pellet. The pellet was resuspended in 4 mL buffer containing RNase. A 4-mL aliquot of a mixture containing NaOH and SDS was then added to the resuspended cells to induce lysis and denature chromosomal and plasmid DNA. The solution was neutralized by the addition of 4 mL of acidic potassium acetate and placed on ice to allow for the precipitation of chromosomal DNA and proteins. The mixture was then centrifuged to pellet the debris and the plasmid-containing supernatant saved. The supernatant was then added to the Qiagen-tip resin column to selectively bind plasmid DNA. The column was washed with 1 M NaCl and the DNA eluted with 1.25 M NaCl at pH 8.5. Isopropanol (3.5 mL) was added to the eluate to precipitate plasmid DNA which was then pelleted by centrifugation. Residual salt was removed by washing the pellet with 70% ethanol. The DNA was then resuspended in TE buffer.

**Restriction digest and gel purification.** To remove the GFP insert, it was cut from pTB93F as a *HindIII* fragment (Fig 5). The high-copy-number plasmid pBS SK+ was cut with *HindIII* as well. Both reactions were loaded onto a 0.9% agarose gel and electrophoresed along with  $\lambda$ -

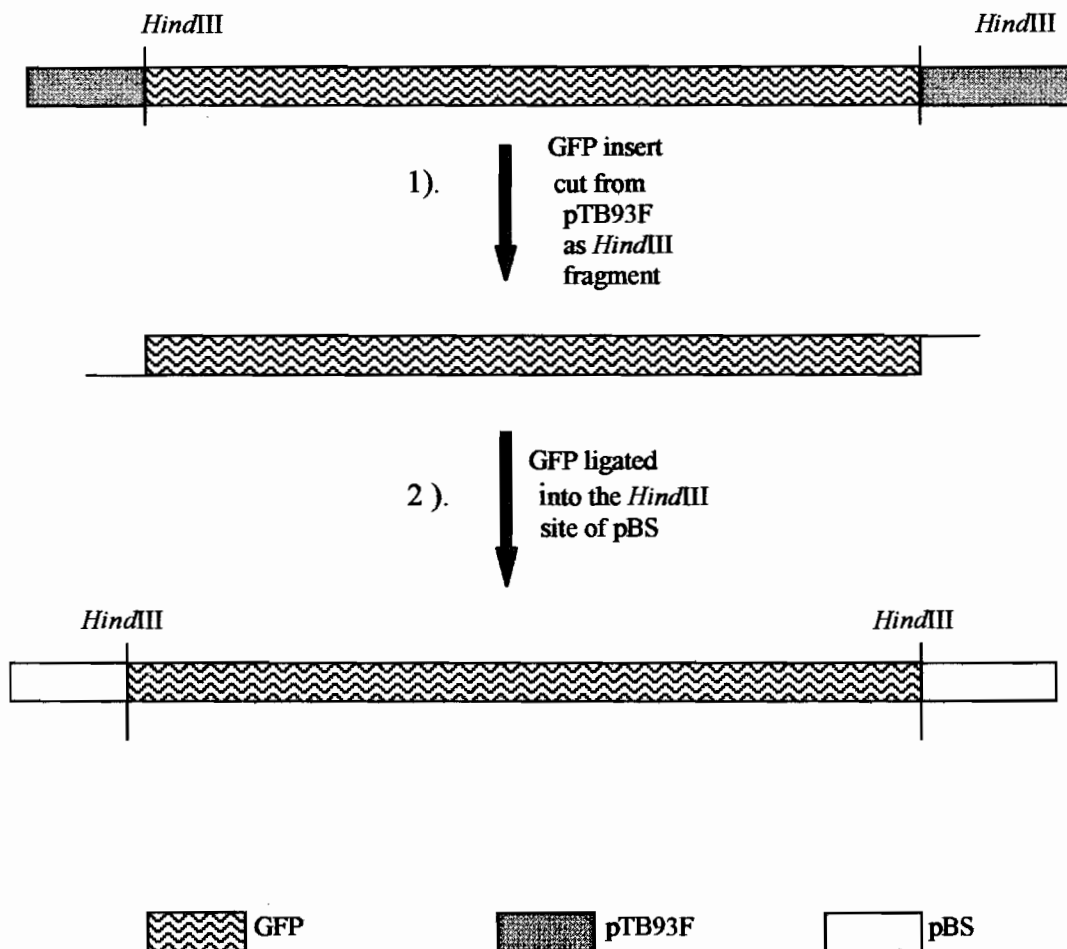
BstEII marker. The bands were visualized by transillumination at 312 nm and excised using a razor blade. DNA was purified from the slices according to the Prep-A-Gene gel purification protocol. The gel slices were placed in a tube and dissolved in the binding buffer provided. A silica-based binding matrix was added to the solution to selectively bind the DNA. The matrix was then pelleted by centrifuging and washed with binding buffer followed by two additional washes with an ethanol-containing wash buffer. Following drying of the pelleted matrix, bound DNA was eluted at 42° C with elution buffer.

**Ligation and transformation.** To insert the GFP fragment into the pBS vector, a ligation reaction was set up. Approximately 50 ng (10  $\mu$ L) of GFP and 10 ng (1  $\mu$ L) of pBS were combined along with ligation buffer and heated at 70° C for 3 minutes to promote dissociation of the complementary overhangs. Ligase and 20mM ATP were added and the reaction incubated at room temperature.

To prepare competent cells, a tube containing 5 mL of LB liquid medium was inoculated with E. coli strain TB1. The culture was incubated at 37° C until cells had reached the mid-log phase of growth, as evidenced by the appearance of turbidity. The cells were pelleted in a clinical centrifuge at 4° C and resuspended in 5 mL of ice-cold 0.1 M CaCl<sub>2</sub>. The cell suspension was placed on ice for 30 minutes. The cells were recovered by centrifuging and concentrated by resuspending in 500  $\mu$ L of 0.1 M CaCl<sub>2</sub>. The tube was placed on ice until needed.

A volume of reaction mixture corresponding to half of the GFP-pBS ligation was added to a tube and diluted with 10 volumes of 0.1 M CaCl<sub>2</sub>. A 100- $\mu$ L aliquot of concentrated cell culture was added to the tube. The mixture of competent cells and DNA was incubated on ice for 30 minutes. Following incubation, the tube was placed in a 42°C heating block for 2 minutes to heat shock the cells and cause them to take up the ligated plasmid DNA. After the addition of 1

mL of LB liquid, the tubes were placed in 37° C incubator for 2 hours. This incubation period allowed the cells to express the Ampicillin-resistance cassette located in pBS. Following incubation, the transformation mixture was plated onto LB agar plates containing ampicillin to select for transformants and X-gal (5-Bromo-4-Chloro-3 Indolyl-B-D-galactoside) to select for plasmid inserts via  $\alpha$ -complementation\*. The plates were incubated overnight at 37° C. Following incubation, colonies containing a plasmid insert, as evidenced by white color, were transferred to a separate plate of LB Amp and grown overnight at 37° C.



\* The plasmid pBS encodes for an  $\alpha$ -fragment which complements the  $\beta$ -galactosidase enzyme of TB1 and restores its ability to breakdown lactose and its analogs. In the case of X-gal, its breakdown results in the production of a blue metabolite which gives the colonies a blue color. In the presence of an insert, this complementing fragment is inactivated and colonies containing such plasmid will appear white.

**Fig. 5.** Outline of the GFP cloning strategy

**Plasmid isolation.** Transferred colonies from the previous step were inoculated into LB Amp liquid and allowed to grow for 12 hours. Plasmid DNA was isolated using the CTAB method. Each culture was transferred to a microfuge tube and centrifuged to pellet the cells which were then resuspended in STET buffer. The resuspended cells were lysed by the addition of lysozyme followed by boiling for 1 minute. Cell debris was pelleted in a centrifuge and discarded. To remove cellular RNA from the lysate, RNase A was added and the mixture incubated at 68° C. At this point, cetyltrimethylammoniumbromide (CTAB) was added to form an insoluble complex with the plasmid DNA. The complex was pelleted by centrifuging. The DNA was released from the CTAB by addition of 1.2 M NaCl and precipitated with 95% ethanol. The plasmid pellet was washed with 70% ethanol to remove excess salts, dried and resuspended in TE buffer.

**Fluorescence analysis.** To confirm active expression of GFP in the transformed TB1 cells, 5 µL of liquid culture was placed on a glass slide with a cover slip. The cells were visualized using a Reichert-Jung Microstar IV fluorescence microscope with an Acridine Orange filter set of 500 nm transmission.

**Insert analysis.** To verify the presence of a GFP insert with isolated plasmid DNA, a quantity of each sample was cut with *Hind III* and electrophoresed. To test for the correct insertional orientation the plasmids were cut with *Pvu II*. The presence of a *Pvu II* site near the end of GFP in addition to 2 within the flanking plasmid DNA enabled this enzyme to be used to screen for insert orientation.

**Site-directed mutagenesis.** A polymerase chain reaction (PCR)-based method of site dir-

ected mutagenesis was used to introduce the mutations leading to blue fluorescence. Specifically, the technique of overlap extension (13, 14) was employed as a general guideline, although some modifications were made. According to the protocol, two primers were designed, one of which was complementary to the sense strand and the other complementary to the antisense strand of the double-stranded GFP gene. Each primer contained within its sequence the desired base change. Additionally, a small overlap was designed into the sequence of the two primers. Primers corresponding to either flanking end of the pBS multiple cloning site (MCS) were also used. The first step involved two reactions. Each reaction contained one mutagenic primer, one flanking primer that annealed to the opposite strand and plasmid template containing the GFP insert. A set of PCR cycles was used to generate two double-stranded, blunt-ended products, each containing the desired mutation. In a third PCR, the two double stranded products from the previous step were placed into a single reaction along with both flanking primers. In this reaction, an overlap-mediated annealing between the two blunt fragments provided two free 3'OH which allowed a subsequent extension to produce a full length gene containing the mutation. The two flanking primers would then selectively amplify this segment (see Fig. 6). The GFP gene could then be recloned into a plasmid and transformed into its bacterial host.

**Phe<sup>64</sup> to Leu.** In order to change the phenylalanine codon, TTC, to a leucine codon, TTG, two mutagenic primers were designed. The sense primer had the sequence 5' ACTACTTTGAC-TTATGGTGTTCAATGC 3'. The antisense primer had the sequence 5' CATAAGACAAAG-TAGTGACAAGTGTT 3'. The mutated base is underlined. The first reactions contained 0.5  $\mu$ M mutagenic primer, 0.5  $\mu$ M T7 forward or T3 reverse flanking primer, 1 U of *Ex Taq*<sup>TM</sup> DNA polymerase, 0.25 mM dNTP mix and 10 ng pBS template with a GFP insert in 1x reaction buffer of 50- $\mu$ L volume. The forward primer reaction (sense strand mutagenic primer) was overlaid

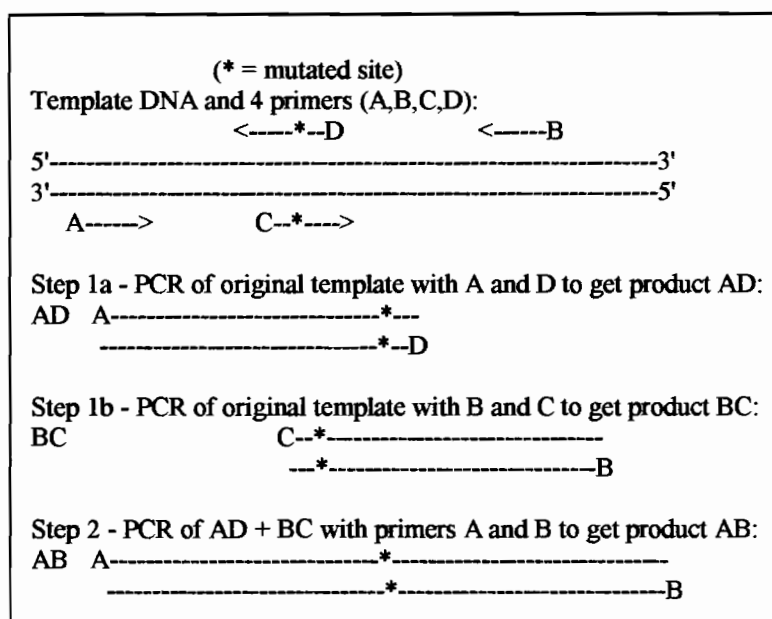


**Fig. 6.** Outline of the site-directed mutagenesis method

with one reaction volume of mineral oil, placed in a Hybaid thermal cycler and amplified as follows: denaturation at 95°C for 30 seconds, annealing at 50°C for 1 minute and extension at 72°C for 1 min for 35 cycles. For the first step, a 2-minute denaturation was used and for the final step, a 10-min extension was used. For the reverse reaction (antisense strand mutagenic primer), amplification was performed as above except for the raising of annealing from 50 to 55° C. The blunt, mutated products from each reaction were analyzed on a 0.9% agarose gel and purified according to the BioRad protocol. They were resuspended in 10 µL elution buffer.

For the second PCR step, the following reaction was set up in triplicate: 20 ng each amplified fragment, 0.5 µM T7 and T3 primers, 1 U ExTaq, and 0.25 mM dNTP mix in 1x reaction buffer with a final volume of 50 µL. PCR conditions were 95°C denaturation for 30 sec with 2 min for the initial stage, 50°C annealing for 1 minute and extension at 72°C for 1 minute with a 10-min

final extension for 35 cycles. The 3 reactions were combined into a single tube and the DNA precipitated at  $-20^{\circ}\text{C}$  with 3 M NaAc and 95% ethanol. The DNA was pelleted in a centrifuge and resuspended in 10  $\mu\text{L}$   $\text{dH}_2\text{O}$ . The entire volume of DNA was loaded onto a 0.9% agarose gel and the GFP band excised and purified using the Prep-A-Gene matrix. The purified GFP containing the F64L mutation was digested with *XhoI* and *PstI*. A 200-ng quantity of pBS was digested with the same two enzymes. The restriction products were gel purified and resuspended in elution buffer. The cut GFP was combined with the cut pBS in a ligation reaction which was incubated overnight at room temperature.

Competent TB1 cells were prepared as described previously. Half of the ligation was transformed into the cells and plated onto LB Amp using blue/white colony screening. The plate was incubated overnight at  $37^{\circ}\text{C}$ . The following day, white colonies were selected and patched onto another LB Amp plate. A CTAB miniprep plasmid isolation was performed as described previously. Isolated plasmid DNA was cut with *HindIII* to confirm the presence of the insert, and with *PvuII* to verify the correct orientation. Transformed cells were viewed under a fluorescence microscope to analyze their phenotype.

**Tyr<sup>145</sup> to Phe.** The mutagenic primers for this procedure were designed to change the tyrosine codon, TAT to the phenylalanine codon, TTT. The sense primer had the sequence 5' ATACAACTTTAACTCACACAATGTATAC 3'. The antisense primer had the sequence 5' TGAGTTAAAGTTGTATTCCAATTTGTG 3'. Mutated blunt fragments were prepared as previously with 0.5  $\mu\text{M}$  mutagenic primer and flanking sequence primer, 0.25 mM dNTP mix, 1 U *Ex Taq* and 20 ng non-mutated GFP plasmid template in 1x reaction buffer with a final reaction volume of 50  $\mu\text{L}$ . Amplification was carried out with  $95^{\circ}\text{C}$  denaturation for 30 sec (2 min initial),  $50^{\circ}\text{C}$  annealing for 1 min and  $72^{\circ}\text{C}$  extension for 1 min (10 min final) for 35 cycles. A 10- $\mu\text{L}$  aliquot

of each reaction was loaded onto a 0.9% agarose gel and purified. The purified fragments (50 ng) were combined for the second step of the mutagenesis along with 0.25 mM dNTP mix, *Ex Taq* and 1x reaction buffer (30  $\mu$ L final). PCR was carried out for 6 cycles with 95° denaturation, 50° C annealing and 72°C extension. At this point the flanking primers T3 and T7 were added (0.5  $\mu$ M final conc) and the reaction volume brought to 50  $\mu$ L. Additional amplification was carried out using standard conditions (95° denaturation, 50° annealing, 72° extension, 35 cycles). Full length, mutated GFP was analyzed on an agarose gel and purified.

Half of the purified Y145F GFP was cut with *HindIII* and the other half was cut with *XhoI* and *PstI*. The two fragments were ligated into pBS cut with the same restriction enzymes. Transformation was carried out as before using competent TB1 *E.coli* and the transformants plated onto LB Amp with X-gal. Transformants containing an insert were patched and inoculated into liquid LB Amp and a CTAB plasmid prep was performed. Insert analysis and fluorescence analysis were performed as well.

**Phe<sup>64</sup> to Leu and Tyr<sup>145</sup> to Phe.** To construct this double mutant, the mutagenic primers for the Y145F mutation were used along with template DNA containing the previously synthesized F64L mutation. The strategy used to produce the Y145F mutation on S65T template was again employed. Mutated DNA was cut with *HindIII*, ligated into pBS and transformed into competent TB1. Plasmid preparation followed by insert analysis and fluorescence microscopy was done.

**Phe<sup>64</sup> to Leu, Tyr<sup>145</sup> to Phe and Tyr<sup>66</sup> to His.** To produce the triple mutant, primers were designed which contained both the F64L and Y66H mutations. The sense primer had the sequence 5' GTCACTACTTTGACTCATGGTGTTC AATGC 3'. The antisense primer had the sequence 5' GCATTGAACACCATGAGTCAAGAGTAG 3'. The first PCR step was performed using the conditions described earlier. For the second step, two strategies were attempted.



Following the first amplification, the product amplified using the T7 forward primer and the sense mutagenic primer was gel purified. The gel purified product was then reamplified in three separate 50  $\mu$ L reactions containing 10 ng of blunt forward product, 0.5  $\mu$ M T7 primer, 0.5  $\mu$ M sense mutagenic primer, 0.25 mM dNTP mix and 1 U *Ex Taq* in 1x reaction buffer. The three reactions were combined in a single tube and precipitated with 0.1 vol. NaAc and 2.5 vol. 95% ethanol.

The precipitated DNA was pelleted in a centrifuge and resuspended in 10  $\mu$ L dH<sub>2</sub>O. The entire volume of resuspended DNA was electrophoresed on a 0.9% agarose gel, and the amplified fragment purified. The megaprimer extension method described by Sarkar and Summer (15) was then used to attempt to generate the full length mutated gene. The amplified blunt fragment containing the mutation was placed in a reaction tube along with along with T3 reverse primer and the full length gene originally used to produce the blunt fragment as template. Thus, the blunt fragment would be used as a PCR primer along with a primer defining the opposite end of the gene. The quantities used were 0.5  $\mu$ M T3 primer, 0.1  $\mu$ M (700 ng) amplified fragment, 10 ng template DNA, 0.25 mM dNTP mix and 1 U *Ex Taq* in 1x reaction buffer for a final volume of 50  $\mu$ L.

A second attempt to produce the full-length mutated gene utilized a modified version of the overlap extension method described earlier. An aliquot of the forward blunt product was reamplified as above and gel purified. Additionally, the reverse blunt product obtained from the amplification using Y145FR primer on F64L template was gel purified. Approximately 30 ng of each were placed into a single 50 $\mu$ L reaction along with 0.5  $\mu$ M of T3 and T7 primers, 0.25 mM dNTP mix and 1 U *Ex Taq* in 1x reaction buffer. Due to the large overlap of these blunt products as a consequence of the distance between the priming sites used to produce them, full-length

product would be generated with higher efficiency. Because both primers contained sequence in the region of the desired mutation and only one contained the mutation, the frequency of mutated product would only be 50%. A small volume of the reaction was analyzed on a gel to verify the formation of product. The remainder of the reaction was then precipitated as before with 0.1 vol. NaAc and 2.5 vol. 95% ethanol, pelleted, resuspended and purified from an agarose gel. The product was cut with *Hind*III and ligated into pBS. The recombinant plasmid was transformed into competent *E. coli* strain TB1 and plated onto LB Amp with X-gal. Colonies containing recombinant plasmids were transferred to a separate plate and inoculated into LB Amp liquid. Plasmid preparation, restriction analysis and fluorescence analysis were performed as before.

## Results

**Purification of GFP from pTB93F.** Following the plasmid midiprep according to the Qiagen protocol, digestion of the plasmid with *Hind*III allowed for the isolation and purification of the GFP insert (Fig. 7). The insert was ligated into pBS cut with the same enzyme and

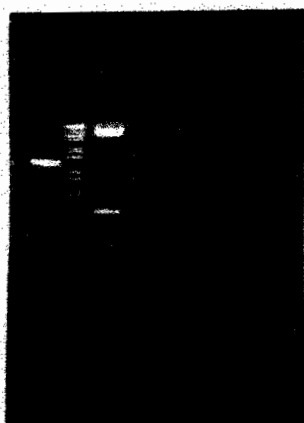


**Fig. 7.** Gel photo of *Hind*III-generated 800 BP GFP fragment (Lane 3). Lane 1 contains pBS cut with *Hind*III. Lane 2 contains  $\lambda$ -*Bst*EII marker.

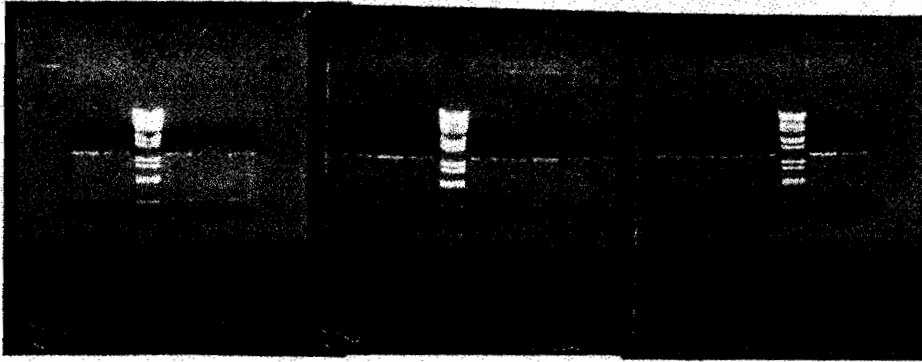
transformed into the TB1 strain of *E. coli*. Based on the number of colonies observed on a con-

control plate, a transformation efficiency of  $7.9 \times 10^5$  transformants/  $\mu\text{g}$  of DNA was calculated. Of the transformants on the experimental plate, 18 white colonies were selected and patched onto another plate of LB Amp. Liquid cell cultures from the patch plate were analyzed microscopically for fluorescence (Table 1). Fluorescence was observed in 6 of the 18 transformants analyzed. To verify that all cells contained the insert, a plasmid miniprep followed by *Hind*III digest was performed (Fig. 8). The presence of an insert in all clones analyzed indicates that

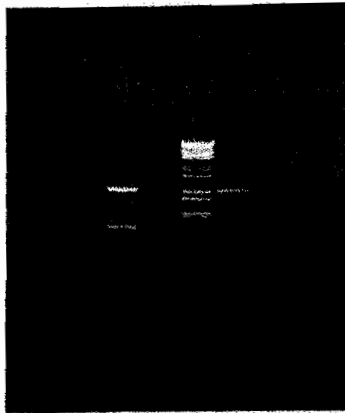
| Sample #    | 1                        | 2                        | 3                        | 4                        | 5                        | 6                        | 7                        | 8                        | 9                        | 10                       | 11                       | 12                       | 13                       | 14                       | 15                       | 16                       | 17                       | 18                       |
|-------------|--------------------------|--------------------------|--------------------------|--------------------------|--------------------------|--------------------------|--------------------------|--------------------------|--------------------------|--------------------------|--------------------------|--------------------------|--------------------------|--------------------------|--------------------------|--------------------------|--------------------------|--------------------------|
| Fluorescent |                          | <input type="checkbox"/> |                          |                          |                          | <input type="checkbox"/> |                          |                          |                          |                          | <input type="checkbox"/> | <input type="checkbox"/> | <input type="checkbox"/> |                          |                          |                          |                          | <input type="checkbox"/> |
| Non-Fluor.  | <input type="checkbox"/> |                          | <input type="checkbox"/> | <input type="checkbox"/> | <input type="checkbox"/> |                          | <input type="checkbox"/> | <input type="checkbox"/> | <input type="checkbox"/> | <input type="checkbox"/> |                          |                          |                          | <input type="checkbox"/> | <input type="checkbox"/> | <input type="checkbox"/> | <input type="checkbox"/> |                          |

**Table 1.** Presence or absence of fluorescence in transformed cells analyzed.

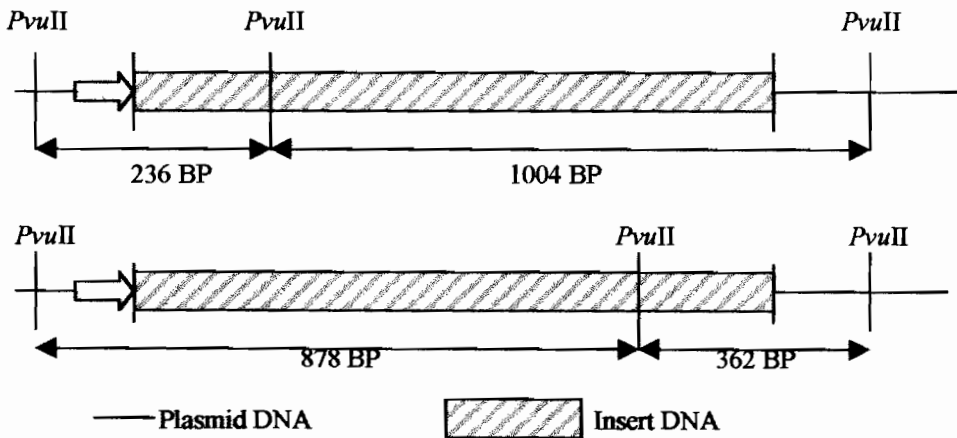
incorrect insert orientation may be responsible for the lack of fluorescence in 12 of the 18 transformants. To test this, a fluorescent (#18) and a nonfluorescent (#10) clone were selected and analyzed by *Pvu*II digestion (Fig. 9). The presence of three *Pvu*II sites within the recombinant plasmid (Fig 10), two in the flanking pBS sequence and one in the GFP insert allowed this enzyme to be used to screen for insert orientation. The insert orientations inferred on the basis of the *Pvu*II fragment sizes observed are consistent with the expression patterns of the two clones. Of these two, clone #18 had an orientation that placed its start codon adjacent to the lac Z promoter of pBS. It is assumed that the other non-expressing clones have the incorrect orientation as well, although the 2:1 ratio of fluorescent to non-fluorescent clones seems difficult to attribute to chance.



**Fig. 8.** Restriction analysis of GFP clones. Gel 1 contains clones 1-5 from left to right. Gel two contains clones 6-12. Gel 3 contains clones 13-18.

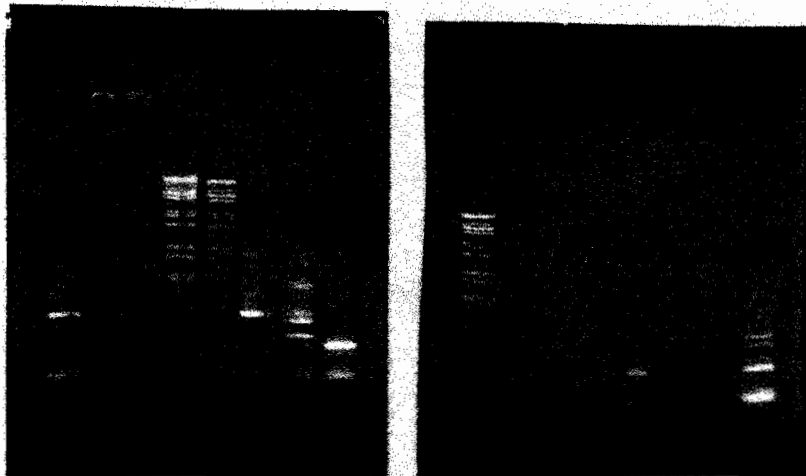


**Fig. 9.** Gel photo of the restriction products of the products of the *Pvu*II digest. Lane 3 contains sample # 18 with bands of 236 and 1004 bases (the largest band is plasmid DNA). Lane 6 contains sample # 10 with bands of 878 and 362 bases.



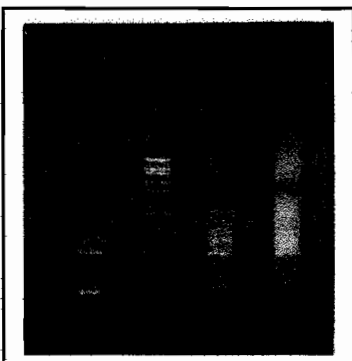
**Fig. 10.** Diagram of the *Pvu*II sites on either side of and within the GFP insert. The orientation which confers expression is indicated at the top. The promoter is shown as a yellow arrow.

**Phe<sup>64</sup> to Leu.** The first step of the Phe<sup>64</sup> to Leu mutation was performed using standard PCR conditions and 50°C annealing. Due to the poor yield of reverse product, a second PCR with 55°C annealing was performed (Fig. 11). The higher annealing temperature was intended to increase the stringency of the hybridization during this step and reduce the amount of product formed through non-specific interactions. With this higher annealing, a considerable enhance-



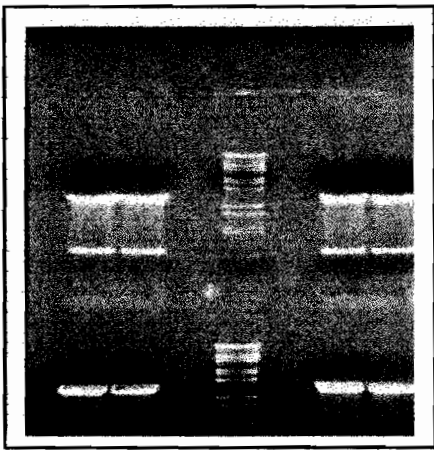
**Fig. 11.** First step of site-directed mutagenesis of F64L. The 650-bp F reaction fragment is located in lane 5 of the gel on the left. The 300-bp R fragment is located in lane 7 (very faint) of the gel on the left and lane 8 of the gel on the right. The latter represents the product of the reaction using 55°C annealing. All other bands are controls.

ment of the target product band was obtained along with a corresponding diminishment of the other bands. The second step of the mutagenic procedure was done in three separate reactions (Fig. 12). These reactions were pooled and the 950-bp final product was purified. This concentration step was necessary as a result of the low yield of product obtained in each reaction.



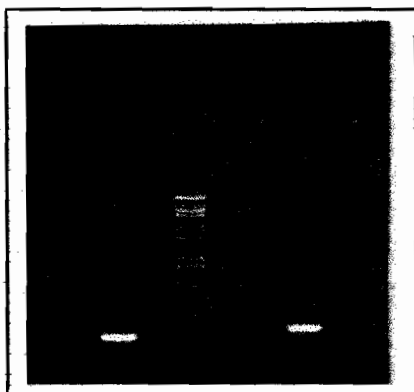
**Fig. 12.** Gel photo of the final PCR product of F64L. The 950-bp fragment in lanes 2, 6 and 8 represents the mutagenized GFP.

Following concentration, the product was cut with *Pst*I and *Xho*I, ligated into pBS and transformed into TB1. Transformation yielded 10 white colonies. Plasmid DNA was isolated from these clones. All selected plasmids contained an insert as was shown by restriction digest of isolated DNA (Fig. 13). Cells from each liquid culture were observed through a fluorescence microscope and shown to emit green light upon excitation at the set wavelength.



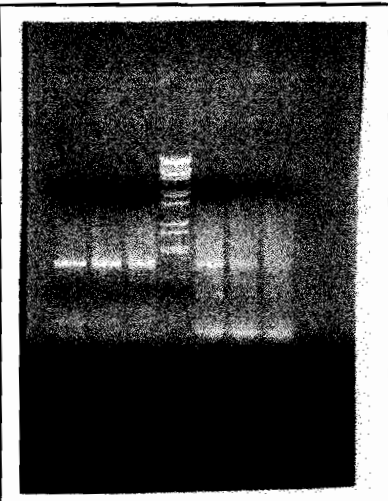
**Fig. 13.** Restriction digest of F64L clones. The insert can be seen as the 850-bp fragment below the plasmid band.

**Tyr<sup>145</sup> to Phe.** The first step of the Y145F mutagenesis procedure was performed, and forward and reverse blunt fragments were obtained (Fig. 14). Due to the high yield of product, no concentration step was necessary. For the second step, standard PCR conditions (95°, 50°, 72° - 35 cycles) were attempted. The absence of any product indicated a problem with the initial extension step. The fact that the overlap region was 75% A-T suggested that weak hydrogen-



**Fig. 14.** The forward and reverse blunt fragments for Y145F. the 509-bp forward fragment is in lane 2 and the 657-bp reverse fragment is in lane 7.

bonding may have been the problem. To address this problem, a series of preliminary cycles with reduced annealing temperatures were added to the PCR program. Additionally, the flanking primers were withheld until after these first cycle. With this alteration, product was obtained (Fig. 15). The DNA was gel purified and divided into two quantities which were cut with *HindIII* or *PstI* and *XhoI*, repurified and ligated into pBS. The recombinant plasmids were trans-

A black and white photograph of a gel electrophoresis image. The gel has seven lanes. Lanes 1, 2, and 3 show a single, bright band of DNA at a specific position. Lanes 5, 6, and 7 also show a single, bright band of DNA at the same position. Lanes 4 and 7 are empty. The bands in lanes 1-3 and 5-7 are of similar intensity, indicating successful PCR amplification in both purified and crude samples.

**Fig. 15.** Gel photo of the Y145F product. Lanes 1-3 contain product obtained using purified forward and reverse blunt fragments. Lanes 5-7 contain product obtained using a crude aliquot of each PCR sample.

formed into TB1.

Three white colonies each were selected from the plates of the *HindIII* and *XhoI-PstI* ligation transformants. The low yield of transformed recombinants is attributable to a low initial concentration of insert DNA. Plasmid DNA was isolated from each transformant and analyzed by *PvuII* digestion (Fig. 16). None of the three clones analyzed from the *XhoI-PstI* ligation contained an insert. These clones probably represent plasmid dimers formed during the ligation. Of the three *HindIII* clones, two contained an insert, and one was of the correct orientation. A liquid culture

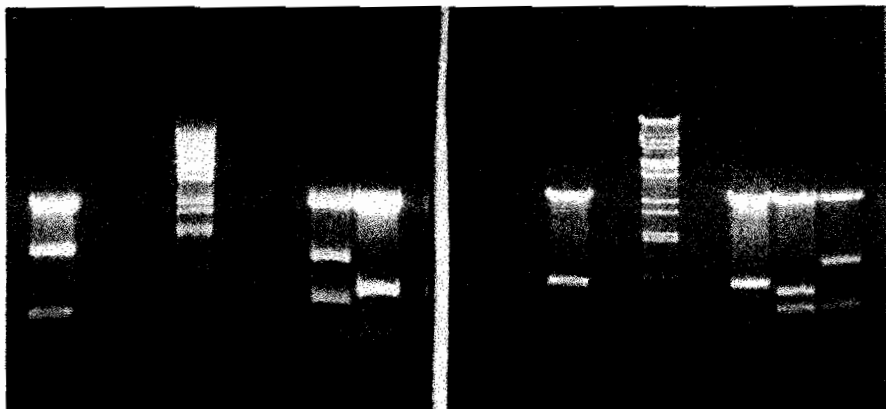


**Fig. 16.** *PvuII* restriction analysis of *HindIII* clones (left) and *XhoI-PstI* clones (right). On the left, lane 1 contains the correctly oriented insert, lane 7 contains an incorrectly oriented insert, and lane 8 contains no insert. On the right, lanes 2, 6 and 7 contain clones with no insert. Lane 8 is a control.

of transformants containing the correctly oriented Y145F insert was analyzed by fluorescence microscopy. At the designated excitation wavelength (475 nm), the cells emitted green light.

**Phe<sup>64</sup> to Leu and Tyr<sup>145</sup> to Phe.** To construct this double mutant, the Y145F mutagenic primers were used along with GFP template containing the F64L mutation. Following the first PCR step (Fig. 17), the blunt fragments were purified and used as template in the second step.



**Fig. 17.** Blunt products from the first step of F64L + Y145F. The 509-bp forward product is in lane 2 and the 657-bp reverse product in lane 7.

Using the modified conditions described for the initial construction of Y145F, approximately 10 ng/ $\mu$ L of full-length product was obtained (Fig. 18). This product was cut with *HindIII*,



ligated into pBS and transformed into TB1. The transformation produced 11 white colonies. The cells from these colonies were patched and inoculated into liquid medium. A CTAB

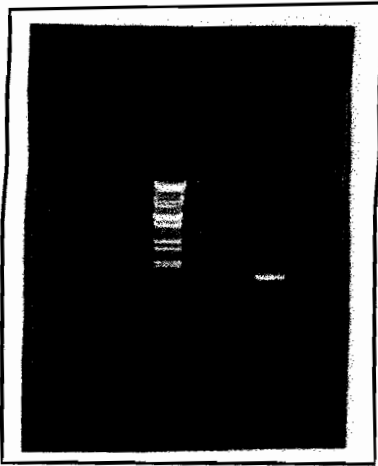


**Fig. 18.** Full-length GFP containing the F64L and Y145F mutations.

plasmid prep followed by *PvuII* restriction analysis was done (Fig. 19). Of 11 the clones, 7 contained a correctly oriented GFP insert. Cells containing these 7 clones were analyzed for

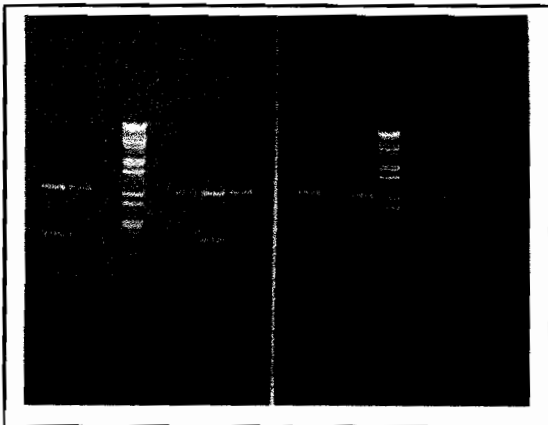


**Fig. 19.** *PvuII* restriction digests of F64L+Y145F clones. In the gel on the left, lanes 1, 2, 7, and 8 contain clones with a correctly oriented insert. On the right gel, lanes 1, 3, and 8 contain correctly inserted clones.

fluorescence. All but one sample of cells had green fluorescence. The incorporation of a spurious mutation during one of the amplification steps may account for the observed lack of fluorescence in one of the samples.

**Phe<sup>64</sup> to Leu, Tyr<sup>145</sup> to Phe and Tyr<sup>145</sup> to His.** To construct this triple mutant, mutagenic primers incorporating the F64L mutation as well as Y66H were used along with template GFP containing the Y145F mutation. In the first PCR, only very weak yields of the reverse blunt fragment and moderate yields of the forward fragment were obtained. In an attempt to generate full-length product without using the reverse fragment, the megaprimer method was employed. The forward fragment was gel purified and reamplified in two separate 50- $\mu$ L and the products concentrated by ethanol precipitation (Fig. 20). Approximately 1 $\mu$ g ( $\sim$  0.5 pmoles) was obtained

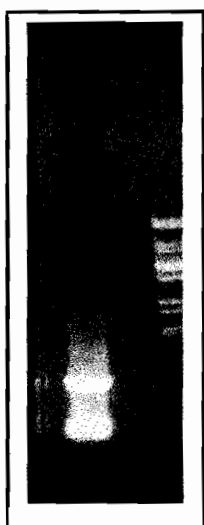


**Fig. 20.** Gel photo of the 650-bp megaprimer.

and used as a forward primer along with T3 reverse primer in a subsequent reaction. The reaction produced no product of the target length. The most likely problem was too small a molar quantity of megaprimer. Because primer concentration is the limiting factor in PCR, an insufficient amount of either primer has the potential to preclude product formation.

A second attempt was made to generate full-length mutant GFP (BFP). In this procedure, purified, reamplified Y66H-F64L forward blunt product was used along with Y145H reverse

blunt product in a second-step mutagenic PCR (Fig. 21). Product of the target length was ob-

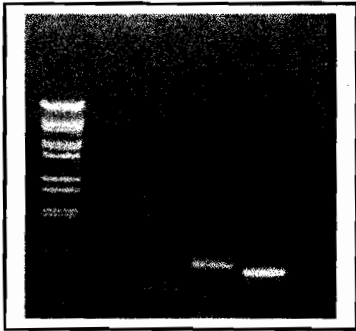


**Fig. 21.** Reamplified Y66H-F64L forward blunt product (lane 4) and Y145F reverse blunt product (lane 5).

tained (Fig 22). This product was concentrated by phenol-chloroform extraction/ ethanol precipitation and cut with *HindIII*. The cut fragment was ligated into pBS and transformed into TB1.

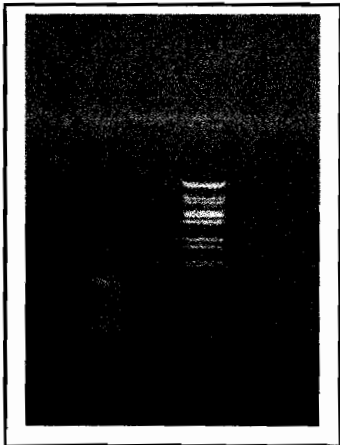


**Fig. 22.** Full-length product obtained using Y145F-R and F64L+Y66H-F.

Following transformation, 14 white colonies were transferred onto another plate and inoculated into LB liquid medium.

Each culture was analyzed under a fluorescence microscope. Due to the nature of the fragments used to generate template in the second mutagenic PCR, only half of the product would be expected to contain the desired mutation. This is a consequence of the fact that both fragments contained sequence in the region to be mutated, but only one contained incorporated the muta-

tion. Because the mutation to be introduced causes a change in emission from green to blue along with a blue-shifting of the absorption spectrum, the two variants generated can be potentially distinguished. Only the green variant would emit at the set wavelength of excitation (475 nm). The absence of fluorescence indicates that either the protein is expressed but fails to undergo excitation or emission at the set wavelengths or the protein is not being expressed due to incorrect insert orientation. The blue-emitting mutants fall into the former category.

The preliminary fluorescence analysis revealed that 2 of the 12 white colonies were positive for green fluorescence and therefore did not contain the mutation. The isolated plasmid DNA was digested with *Pvu*II to determine insert orientation (Fig. 23). The only plasmid DNA con-

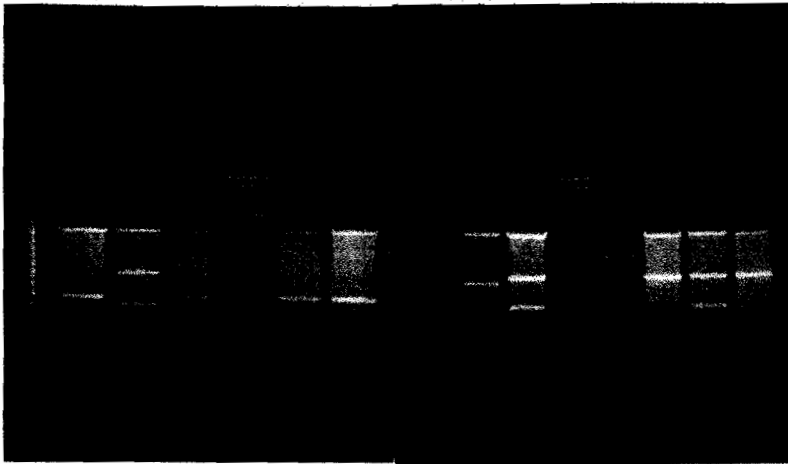


**Fig. 23.** Insert analysis of potential blue fluorescent protein clones. In the gel on the left, lane 2 contains a clone with an incorrectly oriented insert. The clones in lanes 1, 3, 5 and 6 contain no insert. In the gel on the right, lanes 2, 3 and 7 contain clones with an incorrectly oriented insert. The clones in lanes 6 and 8 contain correctly oriented insert and correspond to the green-emitting samples. The clone in lane 1 contains no insert while the clone in lane 5 was not cut during the restriction.

taining correctly oriented insert is that which was purified from the green fluorescent cells.

Sequence analysis of the the insert DNA will be needed to determine which clones, if any, contain the target mutation.

## Discussion

**Summary of codon changes.** The codon changes leading to the production of blue fluorescent protein from wild-type GFP are shown in Figure 24.

|       | 64  | 65  | 66  | 145    |
|-------|-----|-----|-----|--------|
| WTGFP | TTC | TCT | TAT | -- TAT |
| S65T  |     | ACT |     |        |
| F64L  | TTG |     |     |        |
| Y66H  |     |     | CAT |        |
| Y145F |     |     |     | TTT    |

Fig. 24. Codon changes leading to BFP.

**Effects of each mutation.** The blue fluorescent protein (BFP) whose construction has been described here differs from wt GFP by four amino acids. Each substitution has a specific biochemical effect on the fluorophore and consequent alteration of fluorescent properties.

**Ser<sup>65</sup> to Thr.** In wt GFP, the UV-absorbing, non-ionized form of the fluorophore predominates. This lack of ionization of the phenolic hydroxyl group of Tyr<sup>66</sup> is maintained largely by electrostatic repulsion from the nearby charged residue, Glu<sup>222</sup>. The charge on Glu<sup>222</sup> is in turn stabilized by a hydrogen bond with the hydroxyl group of Ser<sup>65</sup>. Upon excitation, as mentioned before, the phenolic hydrogen becomes more acidic and this stimulates its transfer to Glu<sup>222</sup>. The resulting ionization of the fluorophore results in a red-shifting of the excitation spectrum and allows for fluorescent emission. When Thr is substituted for Ser at the 65 position, the extra

methyl group of Thr creates a steric effect which causes the hydroxyl group of this residue to rotate. Upon rotation, its hydrogen bond is transferred from to Val<sup>61</sup> to Glu<sup>222</sup>. At this point, the ionization of Glu<sup>222</sup> is no longer stabilized. The charge now becomes localized on the hydroxyl group of Tyr<sup>66</sup>. With its permanent ionization, excitation occurs exclusively at the red-shifted wavelength (9). With the emitting form as the only conformation, fluorescent intensity increases to 30 times that of the wt. (10). A visual representation of the process can be seen in figure 25.



**Fig. 25.** Comparison of the wt (left) and Ser<sup>65</sup> to Thr (right) fluorophores. The H-bonding of the hydroxyl group of position 65 with Glu<sup>222</sup> (wt) and Val<sup>61</sup> (Ser<sup>65</sup> to Thr) are shown.

**Phe<sup>64</sup> to Leu.** The substitution of Leu for Phe at the 64 position results in the replacement of a bulky side chain with a comparatively small one (Fig. 26). This change alters the steric environment in the region of the fluorophore and improves the folding of the protein. This improved folding leads to enhanced solubility which increases the fluorescent intensity of a sample of GFP (16). Thus, there are no changes in the wavelength of emission or absorption which is consistent with the observations made here.

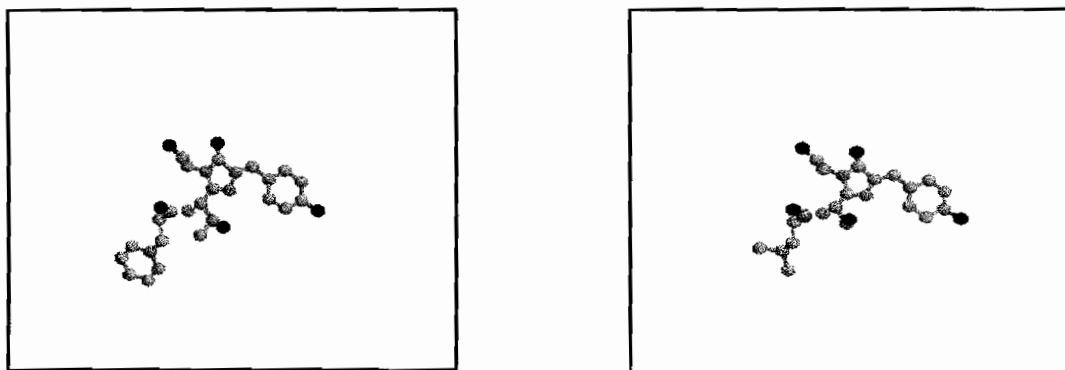


Fig. 26. Comparison of Phe<sup>64</sup> (left) with Leu<sup>64</sup> (right).

**Tyr<sup>66</sup> to His.** The substitution of His for Tyr at this position significantly alters the structure of the fluorophore (Fig. 27). The *p*-hydroxybenzylidene-imidazolidone structure is replaced by imidazole-imidazolidone. The substitution does not appreciably affect the efficiency of form-



Fig. 27. Comparison of the fluorophore before (left) and after (right) the His-66 substitution.

ation of the fluorophore nor does it result in a departure from its planar geometry. The major effects are on the hydrogen bonding of the fluorophore (Fig. 28). With the replacement of the phenol ring with a less bulky imidazole ring, certain residues such as His<sup>148</sup> are able to move

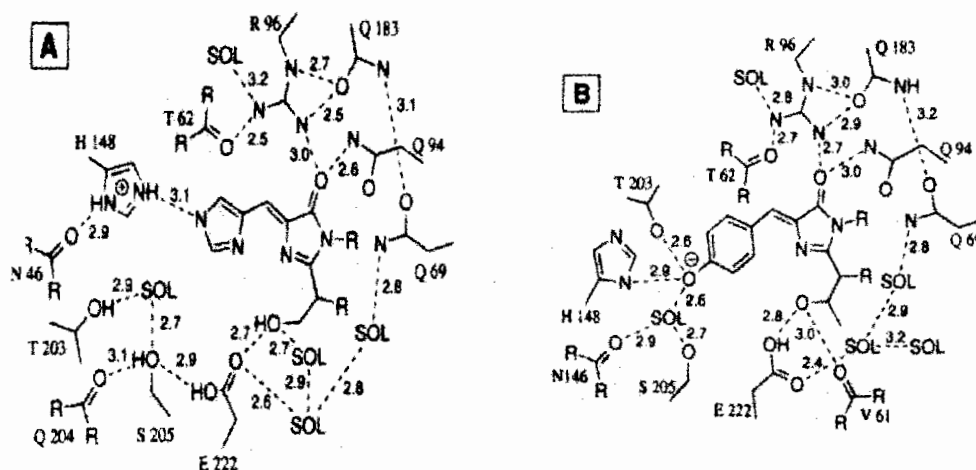


**Fig. 28.** Comparison of the hydrogen-bonding environment of the His<sup>66</sup> fluorophore with that of the Tyr<sup>66</sup> version.

closer to the fluorophore. Additionally, the proton transfer network is eliminated and as a result, the fluorophore is neutral at equilibrium. Spectrally, this fluorophore has a blue-shifted excitation maximum at 382 nm and an emission maximum at the blue wavelength of 448 nm. Fluorescent intensity is considerably less than that of blue variants in part because of an increased extinction coefficient brought about by neutralization of the fluorophore (17).

**Tyr<sup>145</sup> to Phe.** The primary structural difference introduced by this substitution is the removal of a hydroxyl group from the fluorophore vicinity (Fig. 29). Otherwise, the orientation of the benzyl side chain is the same with either residue. The loss of this hydrophilic contact causes a slight alteration in the hydrogen bonding environment and as reported by Heim and Tsien (18) increases the quantum efficiency of fluorescence. Thus, the effect is on intensity of emission rather than wavelength of absorption or emission.





**Fig. 29.** Comparison of Tyr<sup>145</sup> with Phe<sup>145</sup>

The fluorescent analysis of clones containing the mutations at the 64, 65 and 145 positions is consistent with the proposed effects of each substitution. With each of these mutations, excitation is retained in the region of illumination provided by the filter used (475 nm). Additionally, fluorescent emission in the selected range of 505-510 nm is retained. With the His substitution at position 66, these mutations will serve to enhance its fluorescent intensity while retaining the excitation and emission maxima of 382 and 448 nm, respectively. Whereas the substitution of Thr for Ser<sup>65</sup> has a significant effect on the original fluorophore by maintaining its ionization, its effect on the neutral His-containing fluorophore is likely much less. In fact, the effect is most likely limited to slightly increasing the solubility of the protein as reported by Ormö *et al.* (2).

The blue-fluorescing variant of GFP described here will be useful for laboratory work involving bacteria. While there are other BFP's around, the only commercially available form is optimized for human codon usage and would therefore not be suitable for bacteria. In combination with GFP this product has many possible applications.

## Sources Cited

1. Cody, C.W., Prasher, D.C., Westler, W.M., Prendergast, F.G. & W.W. Ward (1993) Chemical structure of the hexapeptide chromophore of the *Aequoria victoria* green-fluorescent protein. *Biochemistry* **32**,1212-1218.
2. Ormö, M., Cubitt, A.B., Kallio, K., Gross, L.A., Tsien, R.Y. & S.J. Remington (1996) Crystal structure of the *Aequoria victoria* green fluorescent protein. *Science* **273**, 1392-1395.
3. Li, X., Zhang, G., Ngo, N., Zhao, X., Kain, S.R. & C.C. Huang (1997) Deletions of the *Aequoria victoria* green fluorescent protein define the minimal domain required for fluorescence. *J. Biol. Chem.* **272(45)**, 28545-28549.
4. Chalfie, M., Tu, Y., Euskirchen, G., Ward & W.W., D.C. Prasher (1994) Green fluorescent protein as a marker for gene expression. *Science* **263**, 800-804.
5. Yang, F., Moss, L.G. & G.N. Phillips (1996) The molecular structure of green fluorescent protein. *Nat. Biotech.* **14**, 1246-1251.
6. Niwa, H., Imouye, S., Hirano, T., Matsumo, T., Kojima, S., Kubota, M., Ohashi, M. & F.I. Tsuji (1996) Chemical nature of the light emitter of the *Aequoria victoria* green fluorescent protein. *Proc. Natl. Acad. Sci. USA* **93**, 13617-13622.
7. Guilbault, G.G. Practical Fluorescence. (Dekker, New York), pp. 6-120.
8. Heim, R., Prasher, D.C. & R.Y. Tsien (1994) Wavelength mutations and posttranslational autooxidation fo green fluorescent protein. *Proc. Natl. Acad. Sci. USA* **91**, 12501-12504.
9. Brejc, K., Sixma, T.K., Kitts, P.A., Kain, S.R., Tsien, R.Y., Ormö, M. & S.J. Remington (1997) *Proc. Natl. Acad. Sci. USA* **94**, 2306-2311.
10. Heim, R., Cubitt, A.B., R.Y. Tsien. (1995) Improved green fluorescence. *Nature* **373**, 663-664.
11. Yang, T.T., Cheng, L. & S.R. Kain (1996) Optimized codon usage and chromophore mutations provide enhanced sensitivity of the green fluorescent protein. *Nucleic Acids Res.* **15**; **24(22)**, 4592-4593.
12. Gage, D.J., Bobo, T. & S.R. Long (1996) Use of green fluorescent protein to visualize the early events of symbiosis between *Rhizobium meliloti* and alfalfa. *Journal of Bacteriology.* **178**, 7159-7166.
13. Ho, S.N., Hunt, H.D., Horton, R.M., Pullen, J.K. & L.R. Pease *Gene* **77**, 51-59.
14. Cormack, B. (1995) *In Short Protocols in Molecular Biology*, Second Edition. (Wiley & Sons, New York), pp: 8.23-8.25.
15. Sarkar, G. & S.S. Sommer (1990) The "megaprimer" method of site-directed mutagenesis. *Biotechniques* **8(4)**, 404-407.
16. Cormack, B.P., Valdivia, R.H & S. Falkow (1996) FACS-optimized mutants of the green fluorescent proein *Gene* **173**, 33-38.
17. Wachter, R.M., King, B.A., Heim, R., Kallio, K., Tsien, R.Y., Boxer, S.G. & S. J. Remington (1997) Crystal structure and photodynamic behavior of the blue emission variant Y66H/Y145F of green fluorescent protein. *Biochemistry* **36**, 9759-9765.
18. Heim, R., and R. Y. Tsien (1996) Engineering green fluorescent protein for improved bightness, longer wavelengths and fluorescence resonance energy transfer. *Curr.Biol.* **6**, 178-182.